

INTERSTITIAL DIFFUSION OF ARSENIC IN SILICON

O. I. VELICHKO

Department of Physics
Belarusian State University of Informatics and Radioelectronics
6 P. Brovka Str.
Minsk, 220013
Belarus
e-mail: velichkomail@gmail.com

Abstract

The mechanism underlying the long-range interstitial migration of nonequilibrium impurity interstitial species was used to simulate arsenic redistribution in ion implantation. An excellent agreement of the calculated arsenic concentration profiles with experimental data allows one to assume that the migration of nonequilibrium arsenic interstitial atoms makes a significant contribution to the formation of a low concentration region on thermal arsenic diffusion. The arsenic concentration profile calculated for a temperature of 1050°C within the framework of this assumption agrees well with the experimental one. A number of parameters describing arsenic diffusion at 1050°C and 1108°C have been obtained.

1. Introduction

Recently, modelling arsenic thermal diffusion has been carried out in [1] on the basis of the diffusion equation

$$\frac{\partial C}{\partial t} = \frac{\partial}{\partial x} \left[D(\chi) h(C, C^B) \frac{\partial C}{\partial x} \right]. \quad (1)$$

Keywords and phrases: arsenic, silicon, interstitial diffusion, modelling.

Communicated by Ana Rosa Silva.

Received March 30, 2016; Revised November 4, 2016

The different cases of concentration dependence $D^C(\chi)$ for the effective arsenic diffusivity $D(\chi)$ represented in the form

$$D(\chi) = D_i D^C(\chi) = D_i \frac{1 + \beta_1 \chi + \beta_2 \chi^2}{1 + \beta_1 + \beta_2}, \quad (2)$$

have been investigated. It is supposed that

$$\chi = \frac{(C - C^B) + \sqrt{(C - C^B)^2 + 4n_i^2}}{2n_i}, \quad (3)$$

$$h(C, C^B) = 1 + \frac{C}{\sqrt{(C - C^B)^2 + 4n_i^2}}, \quad (4)$$

$$D_i = D_i^{E^\times} + D_i^{F^\times} + D_i^{E^-} + D_i^{E^{2-}}, \quad (5)$$

$$\beta_1 = D_i^{E^-} / (D_i^{E^\times} + D_i^{F^\times}), \quad (6)$$

$$\beta_2 = D_i^{E^{2-}} / (D_i^{E^\times} + D_i^{F^\times}). \quad (7)$$

Here C and C^B are the concentrations of substitutionally dissolved arsenic atoms and background impurity of the opposite type of conductivity, respectively; χ is the concentration of electrons, normalized to the intrinsic carrier concentration n_i ; $h(C, C^B)$ is the factor describing the influence of the built-in electric field on the drift of charged pairs; $D_i^{E^\times}$, $D_i^{E^-}$, and $D_i^{E^{2-}}$ are the partial intrinsic diffusivities of dopant atoms due to the interaction with neutral, singly, and doubly negatively charged vacancies, respectively; $D_i^{F^\times}$ is the partial intrinsic diffusivity of arsenic atoms due to the interaction with neutral self-interstitials; β_1 and β_2 are the empirical constants that describe the relative contribution of singly and doubly charged intrinsic point defects to the impurity diffusion.

The empirical constants β_1 and β_2 in expression (2) can be found from the best fit to experimental data. For example, in [2], a fitting routine based on different experimental data was used and the temperature dependences of the arsenic partial diffusivities D_i^\times , D_i^- , D_i^{2-} due to neutral, singly, and doubly negatively charged intrinsic point defects were evaluated. The dependences obtained in [2] allow one to calculate the values of β_1 and β_2 for different temperatures of thermal treatment. It was shown in [1] that the concentration dependence of arsenic diffusivity obtained in [2] provides excellent agreement with experimental data for impurity concentration close to the value of n_i . On the other hand, if the arsenic concentration $C \gg n_i$ and the concentration profile of electrically active arsenic gets a “box-like” form (see Figure 3 in [1]), a difference from the experimental data is observed in the local region where a strong decrease in the impurity concentration begins. Therefore, for solving the problems arising in modelling silicon doping with arsenic it seems more convenient to use the concentration dependence proposed in [3], which is characterized by neglecting the interaction of impurity atoms with doubly charged point defects. Indeed, in this case, good agreement with experiment is observed in the whole region of high impurity concentration and there is only a small difference in the region of low arsenic concentration [1]. It was supposed in [1] that this difference appears due to the direct migration of arsenic interstitial atoms.

The goal of this work is to investigate the possibility of arsenic interstitial diffusion and to obtain complete agreement of modelling results with experimental data.

2. Interstitial Diffusion of Arsenic Atoms in Ion-Implanted Layers

The assumption about the interstitial diffusion of arsenic atoms during ion implantation was first made in [4] with the purpose to explain the experimental data obtained. In [4], the *p*-type Czochralski-grown

silicon substrates of (111) orientation with a resistivity of 5-10 Ω cm were implanted with As⁷⁵ ions at 120keV for doses of 1×10^{12} ions/cm² to 1×10^{16} ions/cm². The average dose rate was approximately 1 μ A/cm². The implantation was carried out at a room temperature with the beam at a 7° angle to the silicon surface in an attempt to minimize channelling. After implantation, the wafers were cleaned and annealed at 600°C-900°C in nitrogen environment. The conductivity profile of the implanted layer was obtained by using the incremental sheet resistance technique. Irvin's well-known data were used to convert the conductivity profile into the electrically active arsenic concentration distribution. It was shown by a special experimental procedure that the "tail" is formed during implantation and not as a result of enhanced diffusion from the high concentration region during the early stages of annealing. Indeed, the main results presented in [4] were obtained for 60 min anneal at 725°C. For the lowest doses, 1×10^{13} ions/cm² and 5×10^{13} ions/cm², annealing at 725°C-1000°C does not affect the profile. At higher doses, the "tail" region remains also unchanged after similar high temperature treatments. The stability of the "tail" indicates that the enhanced diffusion giving rise to its formation occurs either during the implantation or during the early stages of the anneal cycle (< 5 min). In order to demonstrate that the "tail" was formed during the implantation, the entire surface region down to the depth at which the "tail" forms ($\approx 3 \times 10^6 \mu\text{m}^{-3}$) was removed by anodization/stripping after implantation of 5×10^{15} ions/cm² and prior to annealing. After annealing at 600°C, there was no evidence of the electrically active arsenic "tail". When the annealing temperature was increased to 725°C, the "tail" was found to be identical to that observed when the high concentration region was present during annealing. It is concluded, therefore, in [4] that the "tail" forms during implantation and not as a result of enhanced diffusion from the high concentration region during the early stages of annealing. In [4], it was pointed out that the slope of the "tail" is the same for different energies of arsenic

implantation and is also independent of the implantation dose. In addition, when the implant was made through 0.02 μm and 0.06 μm of anodic oxide, a “tail” with the same slope was observed. These results, in particular, the independence of the slope of the “tail” of the amorphous dose limit of 2×10^{14} ions/cm², suggest strongly that the major factor in the “tail” formation is enhanced diffusion during ion implantation and not channelling.

It was mentioned above that after annealing at 600°C, there was no evidence of an electrically active arsenic “tail”. When the annealing temperature was increased up to 725°C, the “tail” became electrically active. The lack of electrical activity at 600°C indicates that the arsenic is not in its usual substitutional environment in the “tail” region. It means that vacancies are not the traps for migrating interstitial species. Indeed, we cannot exclude the heating of the silicon substrate, due to the ion implantation in the experiments of [4], to the temperature sufficient for the point defect diffusion. It follows from the experimental data of [5] that the high energy ion implantation into crystalline Si creates two major damage layers after annealing. The damage in the layer around the average projective range of implanted ions, R_p , is characterized by the domination of self-interstitials, whereas in the layer between the surface and R_p (almost around $R_p/2$) the vacancies are the dominating defect species. This damaged structure is formed due to the spatial separation of implantation-induced vacancies and self-interstitials presumably as a result of the efficient local recombination of primary point defects [6]. Thus, we can suppose that in the “tail” region the interstitial arsenic species are trapped by the defects of interstitial type. If the annealing temperature is higher than 600°C, the arsenic atoms are released from the traps and transfer to the substitutional position. Note that the “tails” are formed in the low concentration region ($< 8 \times 10^6 \mu\text{m}^{-3}$), which is not amorphized, and the lack of electrical activity at a temperature of 600°C is not associated with amorphization.

In Figures 1 and 2, the arsenic concentration profiles measured in [4] after annealing at a temperature of 725°C for 60 minutes are presented. The implantation doses are 5×10^{13} ions/cm² and 1×10^{14} ions/cm², respectively. The chosen values of the doses ensure the maximal impurity concentration below a solubility limit of arsenic in silicon that is equal to $9.85 \times 10^8 \mu\text{m}^{-3}$ for a temperature of 725°C and below an equilibrium electron concentration $n_e = 9.32 \times 10^7 \mu\text{m}^{-3}$ for this temperature [7]. In Figures 1 and 2, we also present the results of modelling the interstitial migration of arsenic atoms during ion implantation. A model of interstitial migration and an analytical solution of diffusion equation proposed in [8] were used for simulation of “tail” formation. Taking into account the results of [4], it was also supposed that the interstitial arsenic species is trapped by uniformly distributed sinks but these sinks are not vacancies. To provide a best fit to experimental data, the Robin’s boundary condition is imposed on the surface of a semiconductor. Use of this boundary condition allows one to describe the evaporation of arsenic interstitial species through the surface.

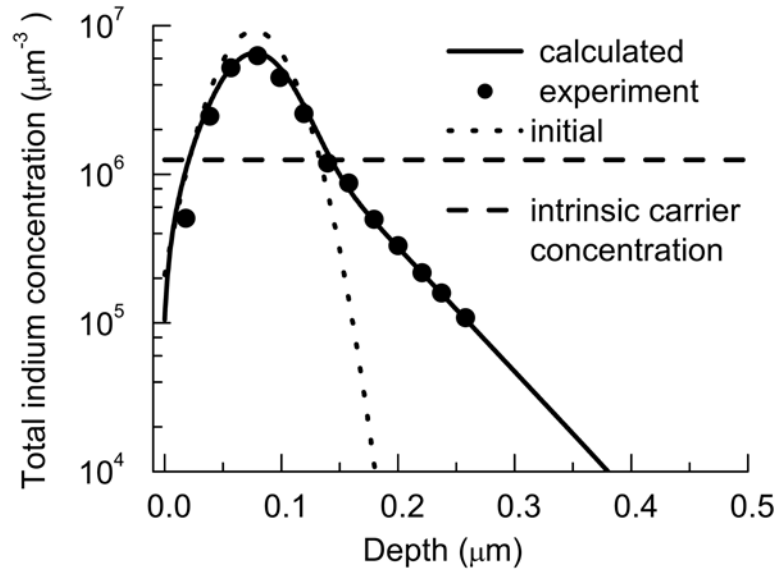


Figure 1. Calculated concentration profile of electrically active arsenic after annealing at a temperature of 725°C for 60 min. Implantation dose equals 5×10^{13} ions/cm². Experimental data are taken from [4]. The dotted curve is the Gaussian distribution after implantation.

The following values of the model parameters were used to provide the best fit of the calculated arsenic concentration profile to the experimental one.

For implantation with the dose $Q = 5 \times 10^{13}$ ions/cm² (Figure 1).

The parameters prescribing the initial distribution of implanted arsenic are: $R_p = 0.077\mu\text{m}$, $\Delta R_p = 0.028\mu\text{m}$. Here R_p and ΔR_p are the average projective range of implanted ions and the straggling of the projective range, respectively. The parameters specifying the process of interstitial diffusion are: the average migration length of arsenic interstitial species $l_{AI} = 0.052\mu\text{m}$, the fraction of the arsenic atoms participating in the interstitial migration $p^{AI} = 50.1\%$.

For implantation with the dose $Q = 1 \times 10^{14}$ ions/cm² (Figure 2).

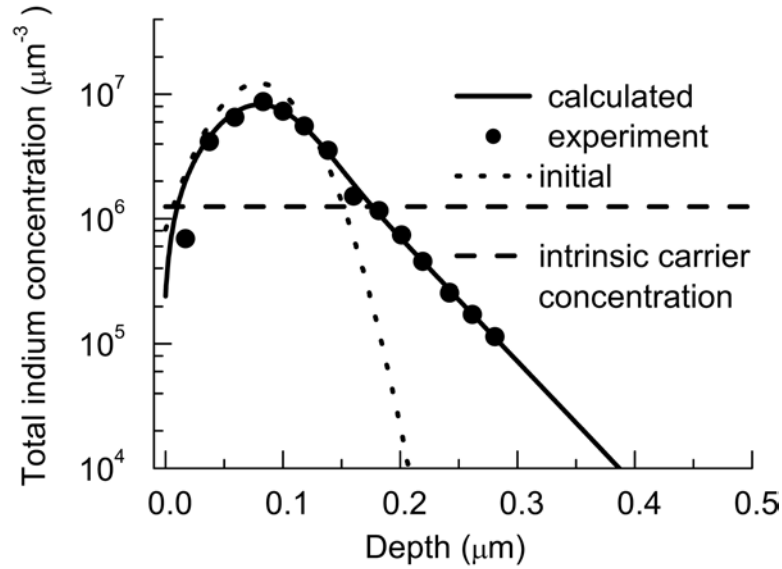


Figure 2. Calculated concentration profile of electrically active arsenic after annealing at a temperature of 725°C for 60 minutes. Implantation dose equals 1×10^{14} ions/cm². Experimental data are taken from [4]. The dotted curve is the Gaussian distribution after implantation.

The parameters prescribing the initial distribution of implanted arsenic are: $R_p = 0.079\mu\text{m}$, $\Delta R_p = 0.034\mu\text{m}$. The parameters specifying the process of interstitial diffusion are: the average migration length of arsenic interstitial species $l_{AI} = 0.044\mu\text{m}$, the fraction of the arsenic atoms participating in the interstitial migration $p^{AI} = 70.4\%$.

It can be seen from Figures 1 and 2 that there is excellent agreement between the calculated arsenic concentration profiles and the electrically active arsenic profiles measured in [4]. The agreement of simulation results with experimental data indicates in favour of the long-range interstitial migration of nonequilibrium arsenic species. It is worth noting that the parameters prescribing the initial distribution of

implanted boron are approximately equal to the values tabulated in [9]: $R_p = 0.0712\mu\text{m}$, $\Delta R_p = 0.0248\mu\text{m}$, $Sk = 0.31$, $R_m = 0.0677\mu\text{m}$. Here Sk and R_m are, respectively, the skewness and the position of a maximum of impurity distribution as implanted which is described by the Pearson type IV distribution [9].

3. Thermal Arsenic Diffusion

It was shown in [1] that the values of intrinsic diffusivity $D_i = 2.55 \times 10^{-6} \mu\text{m}^2/\text{s}$ and the parameters $\beta_1 = 611$ and $\beta_2 = 44.94$ calculated from the expression given in [2] for a temperature of 1108°C provides an agreement with the experimental data [10] for impurity concentration close to the value of n_i . In [10], thermal arsenic diffusion was carried out from a constant source on the surface of a semiconductor. The arsenic concentration profile for 120 min thermal treatment measured in [10] by neutron activation analysis is presented in Figure 3. On the other hand, the results of our simulation of arsenic diffusion based on the model of [3], which neglects doubly charged point defects, give a similar agreement with the experimental data [10]. The following parameters that describe arsenic diffusion were used in this simulation: $D_i = 2.507 \times 10^{-6} \mu\text{m}^2/\text{s}$, $\beta_1 = 100$, and $\beta_2 = 0$ [3]. This agreement is not surprising because the maximal value of χ at the diffusion temperature is equal to 1.78 and $\beta_1\chi \gg \beta_2\chi^2$. Only for $\chi = 13.6$ we have $\beta_1\chi \approx \beta_2\chi^2$. It means that for the diffusion process under consideration a contribution of doubly charged point defects is negligible. Then, due to the great values of β_1 in the models [2] and [3], the arsenic diffusivity can be approximated by the identical expression

$$D(\chi) = D_i D^C(\chi) \approx D_i \chi. \quad (8)$$

In Figure 3, a similar numerical solution of the diffusion equation (1) for the doping process investigated in [10] is also presented. Using a

variation of the parameters D_i and β_1 ($\beta_2 = 0$), we have achieved an ideal fit to the experimental data of [10]. It is worth noting that the obtained values of $D_i = 2.7 \times 10^{-6} \mu\text{m}^2/\text{s}$ and $\beta_1 = 4$, especially β_1 , differ from the values reported in [2] and [3]. Therefore, it is interesting to investigate the arsenic diffusion with a higher doping level. The results of simulation of high concentration arsenic diffusion are presented in Figure 4. The arsenic concentration profile obtained in [10] for a diffusion temperature of 1050°C and duration of 60 minutes is used for comparison.

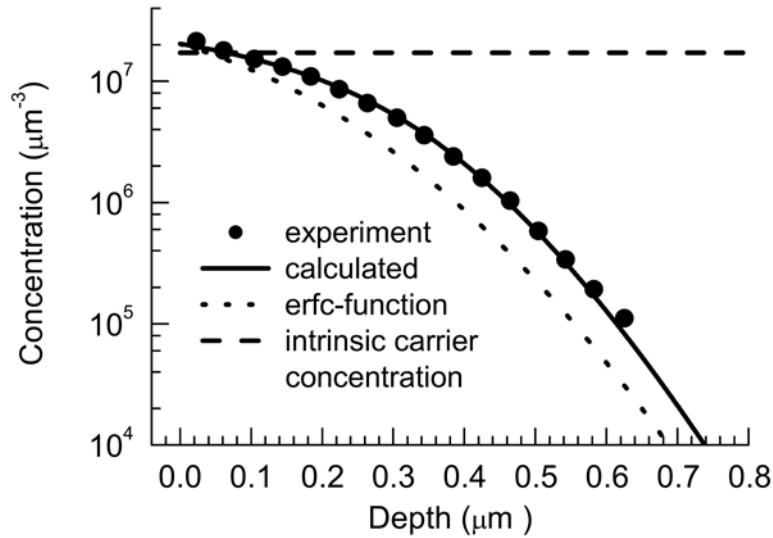


Figure 3. Arsenic concentration profiles formed by thermal diffusion from a constant source on the silicon surface. The solid curve represents the arsenic concentration profile obtained by numerical solution of the diffusion equation that takes account of the concentration dependence of arsenic diffusivity and drift of the charged species in the built-in electric field. Diffusion temperature is 1108°C for 120 minutes. Filled circles are the experimental data of [10].

It can be seen from Figure 4 that the arsenic concentration near the surface is approximately equal to $3 \times 10^8 \mu\text{m}^{-3}$ that results $\chi \approx 18.4$. Thus, arsenic diffusion is characterized by a strong nonlinear concentration dependence of effective diffusivity. On the other hand, arsenic concentration is lower than the maximal equilibrium electron concentration $n_e = 3.566 \times 10^8 \mu\text{m}^{-3}$ for the annealing temperature under consideration [7]. Therefore, it is possible to assume that arsenic clustering does not play an important role in the retardation of diffusion. The values of simulation parameters obtained from the best fitting to the experimental concentration profile are: $D_i = 5.8 \times 10^{-7} \mu\text{m}^2/\text{s}$ and $\beta_1 = 4$ ($\beta_2 = 0$). The impurity concentration at the surface has been chosen equal to $3.2 \times 10^8 \mu\text{m}^{-3}$. It is worth noting that the obtained value of D_i is practically the same as $D_i = 5.8134 \times 10^{-7} \mu\text{m}^2/\text{s}$ calculated for a temperature of 1050°C from the expression proposed in [2]. On the other hand, $\beta_1 = 4$ and $\beta_2 = 0$ used in simulation differ significantly from the values reported in [2]: $\beta_1 = 238.9$; and $\beta_2 = 12.7$. It can be seen from Figure 4 that the calculated arsenic concentration profile described by the dotted curve agrees well with experimental data, except for the region of a low impurity concentration. It is similar to the arsenic profile calculated in [1] within a framework of the model of [3] with $D_i = 5.537 \times 10^{-7} \mu\text{m}^2/\text{s}$, $\beta_1 = 100$, and $\beta_2 = 0$.

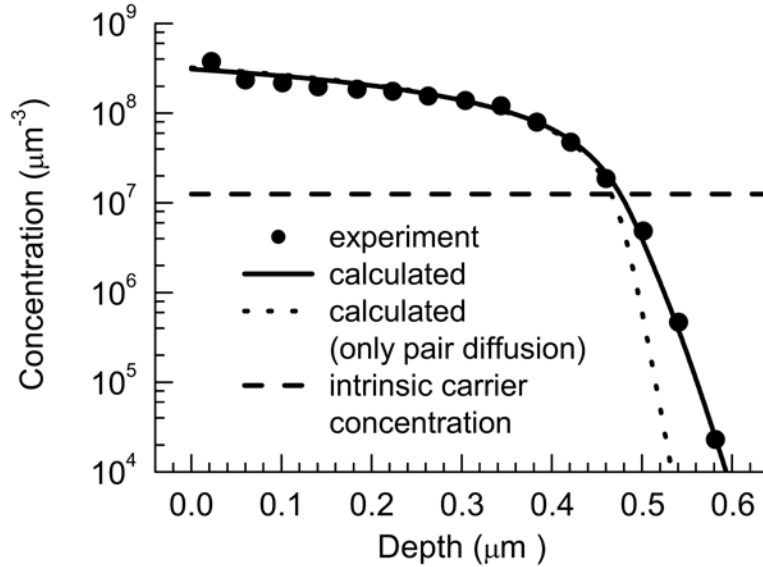


Figure 4. Arsenic concentration profiles formed by thermal diffusion from a constant source on the silicon surface. The dotted curve represents the arsenic concentration profiles obtained by numerical solution of the diffusion equation based on the pair diffusion mechanism. The solid curve takes addition account of the arsenic interstitial migration. Diffusion temperature is 1050°C for 60 minutes. Filled circles are the experimental data of [10].

Taking into account the results obtained, it is reasonable to neglect the contribution of doubly charged point defects in simulation of high concentration arsenic diffusion in silicon, because in this case the calculated profile describes more precisely the high concentration region and the region where a strong decrease in the impurity concentration begins [1]. To achieve the agreement with the experiment in the low concentration region of arsenic distribution, we suppose that generation of nonequilibrium interstitial arsenic atoms can occur during high concentration arsenic diffusion. Participating in the long-range interstitial migration, these atoms form a low concentration region in the arsenic profile. For example, such generation can occur in the region of

the abrupt fall in the arsenic concentration due to the stresses arising in the layer between the highly doped and intrinsic silicon. It is worth noting that in this layer intense dissociation of the “impurity atoms-intrinsic point defect” pairs also takes place, as follows from the mass action law. After dissociation, the arsenic atoms that previously formed pairs become substitutionally dissolved again. However, a small fraction of arsenic atoms can occupy interstitial position and participate in the long-range migration. To take into account this additional impurity flux, the equation for interstitial diffusion [8] can be used. It is worth noting that thermal diffusion of arsenic occurs at temperatures significantly greater than the temperature of ion implantation in the experiments of [4]. Therefore, in contrast to [4], it is supposed in this paper that arsenic interstitials become substitutionally dissolved again via recombination with vacancies (the Frank-Turnbull diffusion mechanism [11]). Then, the system of equations describing arsenic diffusion both by means of the formation, migration, and dissociation of equilibrium “impurity atoms-intrinsic point defect” pairs and due to the long-range migration of nonequilibrium arsenic interstitials has the form:

$$\frac{\partial C}{\partial t} = \frac{\partial}{\partial x} \left[D(x) h(C, C^B) \frac{\partial C}{\partial x} \right] + \frac{C^{AI}(x, t)}{\tau^{AI}} - G^{AI}(x, t), \quad (9)$$

$$d^{AI} \frac{\partial^2 C^{AI}}{\partial x^2} - \frac{C^{AI}(x, t)}{\tau^{AI}} + G^{AI}(x, t) = 0. \quad (10)$$

Here C^{AI} is the concentration of nonequilibrium interstitial arsenic atoms; d^{AI} and τ^{AI} are the diffusivity and average lifetime of these nonequilibrium interstitial atoms, respectively; G^{AI} is the generation rate of arsenic interstitials per unit volume of the semiconductor. We use the stationary diffusion equation for interstitial arsenic atoms in view of their large average migration length $l_{AI} = \sqrt{d^{AI}\tau^{AI}}$ and small lifetime ($\tau^{AI} \ll \tau_p$), where τ_p is the duration of thermal treatment.

A numerical solution of the system of diffusion equations (9) and (10) for the process investigated in [10] is presented in Figure 4 by a solid curve. It can be seen from Figure 4 that account of the migration of nonequilibrium arsenic interstitials allows one to explain the formation of the “tail” in the low concentration region and to achieve complete agreement of the arsenic concentration profile with the experimental one. The values of the simulation parameters that provide the best fit to the experimental concentration profile are: $D_i = 6.2 \times 10^{-7} \mu\text{m}^2/\text{s}$ and $\beta_1 = 4$ ($\beta_2 = 0$). The impurity concentration at the surface C_S has been chosen equal to $3.1 \times 10^8 \mu\text{m}^{-3}$ and the average migration length of nonequilibrium arsenic interstitials $l_{AI} = 0.013 \mu\text{m}$. It can be seen from Figure 4 that the calculated arsenic concentration profile described by the solid curve agrees well with experimental data over the whole diffusion zone. It is worth noting that full agreement with the measured concentration profile has been achieved using the assumption of the long-range migration of nonequilibrium arsenic interstitials. This assumption is based on the results of the previous simulation of arsenic diffusion during ion implantation. On the other hand, there can be another way to describe the low concentration “tail” region of arsenic distribution. For example, it was shown in [12] that in the low concentration region a condition of a local thermodynamic equilibrium between the substitutionally dissolved impurity atoms, intrinsic point defects, and “impurity atom-intrinsic point defect” pairs can be broken up. In this case, the nonequilibrium pairs will be playing the role of nonequilibrium arsenic interstitials. Moreover, it was shown in [13] that a similar “tail” region can be formed in the case of diffusion of equilibrium “impurity atom-intrinsic point defect” pairs if the non-uniform distribution of intrinsic point defects in the neutral charge state arises. Such non-uniform distribution can be formed due to the intense dissociation of “impurity atoms-intrinsic point defect” pairs in the region of abrupt fall of arsenic concentration.

As follows from the results of modelling, the average migration length of arsenic interstitials in ion implanted layers (0.052 μm and 0.044 μm) differs from that obtained for the thermal diffusion (0.013 μm). We can explain this difference as a corollary of the difference in the trapping mechanisms of arsenic interstitials. Indeed, the “tail” in the ion-implanted layers is located in the region of interstitial defects, created by implantation, that interact with the migrating arsenic interstitials. On the other hand, it is supposed in the case of thermal diffusion that the arsenic interstitials recombine with the vacancies. The vacancy concentration is significantly increased with temperature. As a result, the average migration length of arsenic interstitials is smaller for high temperature thermal doping.

It is interesting to note that within the framework of arsenic interstitial generation due to the elastic stresses, the absence of interstitial diffusion in the low doped layers is explained naturally. Indeed, in these layers there are no lattice mismatch and, respectively, no significant stresses between the doped region and undoped substrate. Then, the generation of arsenic interstitials is also negligible. We can also explain the absence of interstitial diffusion in the low doped layers if the generation of arsenic interstitials occurs due to the intense dissociation of the “impurity atoms-intrinsic point defect” pairs in the region of the abrupt fall in the arsenic concentration. Indeed, let us suppose that the arsenic interstitials are generated due to dissociation of the pairs of an arsenic atom with a singly charged point defect. The concentration of these pairs is significantly increased in a highly doped layer. Therefore, the concentration of arsenic atoms that occupy the interstitial position and participate in the long-range migration also increases.

4. Conclusion

On the basis of the mechanism of the long-range interstitial migration of nonequilibrium impurity interstitial species, simulation of arsenic concentration profiles measured in [4] after implantation and annealing of silicon substrates at a temperature of 725°C for 60 minutes has been carried out. The arsenic concentration profiles calculated for ion implantation with an energy of 120keV and doses of 5×10^{13} ions/cm² and 1×10^{14} ions/cm² agree well with experimental ones. Thus, the simulation results obtained confirm the assumption of [4] that the “tail” in the low concentration regions of arsenic profiles is formed due to the interstitial migration of arsenic species during ion implantation. The average migration length of arsenic interstitial species obtained from the best fit to the experimental concentration profiles are equal to 0.052μm and 0.044μm for implantation with doses of 5×10^{13} ions/cm² and 1×10^{14} ions/cm², respectively.

Based on the results obtained, simulation of thermal arsenic diffusion has been carried out. It is shown that assumption of the long-range migration of nonequilibrium arsenic interstitial atoms allows one to explain the formation of the “tail” in the low concentration region for the case of high concentration arsenic diffusion. Complete agreement of arsenic concentration profile with the experimental one [10] has been achieved over the whole diffusion zone. The average migration length of nonequilibrium arsenic interstitials obtained from the best fit to the experimental concentration profile is equal to 0.013μm. It is worth noting that the empirical parameter β_1 that describes the relative contribution of singly charged intrinsic point defects to the impurity diffusion is equal to the same value for diffusion at temperatures of 1108°C and 1050°C. The value of $\beta_1 = 4$ obtained from the best fit to the experimental arsenic profiles differs significantly from the values used in [2] and [3].

References

- [1] O. I. Velichko, On concentration dependence of arsenic diffusivity in silicon, *Int. J. Comp. Mat. Sci. Eng.*, Art. No. 1650005 [10 pages] (2016).
doi:10.1142/S2047684116500056
- [2] A. Martinez-Limia, P. Pichler, C. Steen, S. Paul and W. Lerch, Modeling of the diffusion and activation of arsenic in silicon including clustering and precipitation, *Solid State Phenom.* 131-133 (2008), 277-282.
- [3] M. Y. Tsai, F. F. Morehead, J. E. E. Baglin and A. E. Michel, Shallow junctions by high-dose As implants in Si: experiments and modeling, *J. Appl. Phys.* 51(6) (1980), 3230-3235.
- [4] F. N. Schwettmann, Enhanced diffusion during the implantation of arsenic in silicon, *Appl. Phys. Lett.* 22(11) (1973), 570-572.
- [5] A. Peeva, R. Kögler, W. Skorupa, J. S. Christensen and A. Yu. Kuznetsov, Spatial distribution of cavities in silicon formed by ion implantation generated excess vacancies, *J. Appl. Phys.* 95(9) (2004), 4738-4741.
doi:10.1063/1.1690095
- [6] P. Lévêque, H. K. Nielsen, P. Pellegrino, A. Hallén, B. G. Svensson, A. Yu. Kuznetsov, J. Wong-Leung, C. Jagadish and V. Privitera, Vacancy and interstitial depth profiles in ion-implanted silicon, *J. Appl. Phys.* 93(2) (2003), 871-877.
doi:10.1063/1.1528304
- [7] S. Solmi, Dopants in silicon: Activation and deactivation kinetics, in: "Encyclopedia of Materials: Science and Technology", edited by K. H. J. Buschow, R. W. Cahn, M. C. Flemings, B. Ilshner, E. J. Kramer, S. Mahajan and P. Veyssi re (Elsevier Science Ltd., 2001), 2331-2340.
- [8] O. I. Velichko and N. A. Sobolevskaya, Analytical solution of the equations describing interstitial migration of impurity atoms, *Nonlinear Phenom. Complex Syst.* 14(1) (2011), 70-79.
- [9] A. F. Burenkov, F. F. Komarov, M. A. Kumakhov and M. M. Temkin, *Tables of Ion Implantation Spatial Distributions* (Gordon & Breach Science Publ.; Rev. Enl. Edition, 1986), 462 p.
- [10] T. I. Chiu and H. N. Ghosh, A diffusion model for arsenic in silicon, *IBM J. Res. Develop.* 15(6) (1971), 472-476.
- [11] F. C. Frank and D. Turnbull, Mechanism of diffusion of copper in germanium, *Phys. Rev.* 104 (1956), 617-618.

<http://dx.doi.org/10.1103/PhysRev.104.617>

- [12] O. I. Velichko, Narushenie uclovija lokalnogo termodinamicheckogo ravnovecija pri b'ictr'ih termicheckih otjigah ionno-implantirovannogo kremnija (Violation of the condition of local thermodynamic equilibrium on rapid thermal annealing of ion-implanted silicon) Radiotekhnika i Elektronika (Radioengineering and Electronics) Republican interdepartmental volume of papers, Minsk, Belarus, 15 (1986), 106-110 (in Russian).
- [13] O. I. Velichko, Mechanism of locally enhanced diffusion of impurities under condition of high concentration doping of silicon with phosphorus, Elektronnaya tehnika. Ser. 2, Poluprovodnikovie pribory (Electronic Engineering, Part 2, Semiconductor Devices), 2(187) (1987), 57-63 (in Russian).

